

AD-A217 600

Submitted to IEEE-JQE

Special Issue on Tunable Solid State Lasers

DTIC FILE COPY

Growth, Spectroscopy and Lasing of Titanium-Doped Sapphire

P. Lacovara and L. Esterowitz
Naval Research Laboratory

M. Kokta
Union Carbide Corp.

N00014-85-C-2143

ABSTRACT

The growth, spectroscopy and lasing of titanium-doped sapphire are discussed. Particular attention is given to the problems of achieving high quality laser material and to the identification and elimination of defects that currently limit $\text{Ti:Al}_2\text{O}_3$ laser performance.

DTIC
ELECTE
JAN 31 1990
S E D

DISTRIBUTION STATEMENT A

Approved for public release;
Distribution Unlimited

90 01 26 027

Exhibit D

STATEMENT "A" per Dr. L. Esterowitz
NRL, Code 6550
TELECON

1/31/90

CG

Growth, Spectroscopy and Lasing of Titanium-Doped Sapphire

P. Lacovara and L. Esterowitz
Naval Research Laboratory
Code 6550
Washington, D. C., 20375

M. Kokta
Union Carbide Corporation
750 S. 32nd Street
Washougal, WA 98671

Accession For	
NTIS GRA&I	<input checked="" type="checkbox"/>
DTIC TAB	<input type="checkbox"/>
Unannounced	<input type="checkbox"/>
Justification	
By	
Distribution/	
Availability Codes	
Dist	Avail and/or Special
A-1	

The announcement of efficient, broadly tunable laser action in titanium-doped sapphire¹ has inspired considerable work. Experiments at NRL², and elsewhere³ have demonstrated successful lasing using both flashlamp and laser pumping. Crystal quality, however, is in great need of improvement, since loss within the material is as much as an order of magnitude greater than would be expected for high-quality sapphire. In this paper we discuss some of the problems associated with the growth of this material and point out their effect on laser performance. We also show some areas where the spectroscopy of this material is not well understood, and propose some explanations for these spectroscopic features.

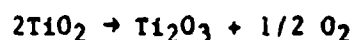


I. Growth

Growth of titanium-doped sapphire ($\text{Ti}:\text{Al}_2\text{O}_3$) has been achieved using the heat-exchanger method, the flame-fusion method and the Czochralski method. The samples used in this work were grown by the latter technique, using an inductively heated iridium crucible in zirconia insulation. The atmosphere over the crucible was pure N_2 . Growth was initiated by touching an oriented sapphire seed onto the top of the melt.

The pull rate was typically 0.5 cm/hr, with diameter control achieved by constantly measuring the weight of the growing crystal.

The crucible charge used in growing Ti:Al₂O₃ typically consists of TiO₂ and Al₂O₃, with the latter either in pressed pellets or in crackle form (pure sapphire grown by the flame-fusion method). Above approximately 1750°C, TiO₂ undergoes a dissociation to Ti₂O₃ (Ti³⁺) via the reaction



The liquid Ti₂O₃ then reacts and mixes with the molten Al₂O₃ upon reaching 2050°C. The miscibility of Ti₂O₃ in molten Al₂O₃ is small, not exceeding 1% by weight, posing part of the difficulty in achieving quality crystals of high concentration. The distribution of Ti³⁺ between the crystal and the melt may be modeled by

$$C_s = KC_0 \left(1 - \frac{W_s}{W_l}\right)^{K-1}$$

where "C₂" is the dopant concentration in the solid, "C₀" is the initial dopant concentration in the melt, "W_s" is the weight of the crystal, "W_l", is the weight of the charge, and "K" is the distribution coefficient between the solid and the liquid. The value of "K" varies depending on growth conditions, and in particular on the crystallization rate. The smallness of "K" is due in large part to the substantial mismatch between the ionic radius of Ti³⁺ and Al³⁺. By pulling at a very small rate (~0.025 cm/hr), crystals may be obtained with concentrations approaching approximately 0.24

weight percent of titanium; however, at concentrations above about 0.1%, absorption loss at laser wavelengths becomes unacceptable, so that our most successful laser work has been obtained using rods at a nominal 0.1% concentration.

The substitution of Ti^{3+} into Al_2O_3 presents some interesting contrasts to the substitution of Cr^{3+} in ruby. If we compare the ionic radius in sixfold coordination⁴ of Al^{3+} to that of Ti^{3+} , we find a 26% increase from adding the d^1 electron to the closed (p^6) shell (0.53 Å for Al^{3+} versus 0.67 Å for Ti^{3+}). Ionic radius decreases (for constant coordination and valence) along the 3d transition series⁴, so that at chromium (d^3) $R^{3+} = 0.61$ Å. The substitution of Ti^{3+} is thus substantially more perturbative to the lattice than the similar substitution of Cr^{3+} in ruby. It is likely that Ti^{3+} distorts its local environment into closer resemblance with the isomorphous structure Ti_2O_3 , which has a unit cell⁵ about 13% bigger than that of Al_2O_3 . This distortion can be seen in studies of low concentrations of Ti^{3+} in Al_2O_3 , where an increase in lattice parameter is observed⁶, and in the graphic demonstration afforded by boules of $Ti:Al_2O_3$ which shatter during growth due to the incorporation of excess titanium⁷. A more subtle difference is that of crystal field stabilization energies^{8,9}. The crystal field stabilization energy (c.f.s.e) may be thought of as the reduction in ground state energy of the incorporated ion compared to that of the free ion due to the crystal field splitting of the degenerate electronic states (the usual Tanabe-Sugano diagram disguises this fact, since by convention the ground state energy is plotted with zero slope). Because of differences in the

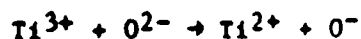
splitting parameter Dq and splitting patterns for different symmetries, there will in general be a difference in c.f.s.e. for the same ion in sites of different symmetry, aside from the larger differences in lattice energy. Usually large lattice effects dominate, but it often is necessary (as in the case of normal and inverted spinels¹⁰) to include c.f.s.e. In the general case, we find the ratio of c.f.s.e. for octahedral versus tetrahedral sites to be about 3:2 for Ti^{3+} ($2D$ free ion ground state), compared with 9:2 for Cr^{3+} ($4F$ free ion ground state). For the crystal field strength of sapphire, the difference in c.f.s.e. for particular ions, the "octahedral site preference energy"¹¹, is only about 0.33 eV per ion for Ti^{3+} , but 2.0 eV for Cr^{3+} . The large site preference energy for Cr^{3+} in part explains the usual occurrence of Cr^{3+} in six-fold coordination in complexes, glasses, and crystals. The implication for Ti^{3+} is that a non-trivial fraction of Ti^{3+} ions might be incorporated into defect or interstitial sites of low symmetry during growth. After-growth annealing would be expected to relax some of these ions into octahedral sites.

II. Spectroscopy

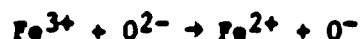
The absorption and fluorescence spectra of $Ti:Al_2O_3$ are to first approximation what would be expected from a d^1 ion in an octahedral crystal field¹². There are, however, complications to these spectra which have a direct bearing on the lasing characteristics of $Ti:Al_2O_3$. We begin by discussing the features of the absorption and fluorescence spectra which are easily explained, and then consider the ultraviolet and infrared absorptions which accompany them.

The blue-green absorption band of $\text{Ti:Al}_2\text{O}_3$ is due to the vibronically broadened ${}^2\text{T}_2 \rightarrow {}^2\text{E}$ transition¹³. The double hump is due to a static Jahn-Teller distortion¹² of the E state which splits the excited state by nearly 2000 cm^{-1} . The ${}^2\text{T}_2$ state is actually split into $\text{A}_1 + \text{E}$ by the trigonal component of the crystal field but since this is less than the Jahn-Teller splitting¹³ we will ignore it for the time being. Since the cation site lacks inversion symmetry (the site symmetry is rigorously C_3 rather than O_h for the center of a regular octahedron), the crystal field mixes odd parity states with the even parity d orbitals, relaxing the forbiddenness of the even to even parity transition. As a result, electric dipole transitions are allowed, and the absorption and fluorescence bands of $\text{Ti:Al}_2\text{O}_3$ are fairly strong ($\sigma \sim 10^{-20}\text{ cm}^2$), and largely independent of temperature¹⁴. The fluorescence band peaks at about 760 nm, with a fluorescent lifetime of about 4 μsec .

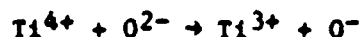
The next obvious feature in the absorption spectrum of $\text{Ti:Al}_2\text{O}_3$ is the strong charge transfer¹⁵ absorption which sets in below 300 nm. Because the charge-transfer absorption satisfies both spin and parity selection rules, it is strongly electric dipole allowed, with an oscillator strength ~ 0.1 .¹⁵ This strong absorption makes the observation of structure within the band using crystals of moderate dopant concentration and reasonable thickness very difficult. Tippins¹⁰ has studied the charge-transfer bands of titanium (and other transition metals) in Al_2O_3 , using low concentrations and thin samples. Tippins' spectrum of $\text{Ti:Al}_2\text{O}_3$ assigns a hump in the UV absorption between 5.5 and 8 eV to the charge-transfer



in good agreement with simple theory. A weakened hump appears between approximately 4.5 and 5 eV is assigned to the charge transfer



This analysis does not prove entirely satisfying, since the measured content of iron in our $\text{Ti}:\text{Al}_2\text{O}_3$ samples is less than one part-per-million, smaller by more than an order of magnitude than that required for the observed absorption. The spectra of Ferguson and Fielding¹⁸, and Lehman and Hardon¹⁹, taken in thicker, higher doped crystals, show much stronger absorption, but without sufficient resolution in the area of 300 nm to properly resolve this question. Recently experiments^{20,21} duplicating Tippins' measurements on $\text{Ti}:\text{Al}_2\text{O}_3$ have also raised questions regarding the proper assignment of the absorption around 300 nm. A charge transfer of the type



was proposed. An experiment in which crystals of accurately known dopant and extraneous impurity concentrations are used to study the region around 300 nm would go a long way towards putting this issue to rest. Ultra-violet pumping of $\text{Ti}:\text{Al}_2\text{O}_3$ samples gives two strong fluorescence bands, one peaked around 425 nm, the other around 575 nm (Fig. 1). The excitation bands for these emissions are broad but discrete, peaking around 250 nm, and 310 nm, respectively, suggesting two types of point defect (color) centers^{22,23}. Considering the strength of the color center fluorescence, at least part of the anomalous UV absorption is certainly due to color center absorption.

The spectroscopic feature with which we are most concerned is the broad IR absorption observed in $\text{Ti}:\text{Al}_2\text{O}_3$. This absorption peaks at approximately 750 nm but extends with considerable strength over the entire

Ti:Al₂O₃ fluorescence band. The band is most pronounced in crystals at higher doping levels, and its strength grows quickly with doping. For example, unannealed samples of 0.1 and 0.2 weight percent titanium grown under identical conditions are found to have peak absorptions of 2%/cm and 13%/cm, respectively.

Absorption by iron impurities¹⁸ is a possible cause for this feature. Sapphire containing an iron concentration of approximately 5×10^{-4} would partially account for the placement and the breadth of the absorption; this explanation must, however, be rejected for several reasons. The most obvious is that the concentration of iron in our samples is roughly 3 orders of magnitude too small to account for the measured absorption coefficient. In addition, the iron absorption would show a marked (factor of 3) increase in absorption between light polarized parallel and perpendicular to the c axis, respectively. No large change in absorption is seen in our Ti:Al₂O₃ samples. The assignment of this band in iron doped sapphire to an Fe³⁺-Fe²⁺ charge transfer speaks against this strong absorption for such a dilute impurity. Absorption by Ti³⁺ pairs must also be rejected because of the low dopant concentration, and the success of after growth treatment in reducing the band. Absorption by Ti²⁺ has also been raised as a possibility. Aside from the large size⁴ of this ion ($R = 0.86 \text{ \AA}$), Ti²⁺ is so strongly reducing that it would not be expected to form during growth, much less remain divalent. Since Ti²⁺ is isoelectronic with V³⁺, the spectrum of this ion should resemble that of the latter, shifted to lower energy by perhaps 50% because of the reduction in Dq with the reduced ionic charge and the change in Racah parameters. This would give a double-humped band¹³ in the right

location, but with strong polarisation dependence. Other transition metal impurities must be ruled out because of their low concentration, and the lack of accompanying spectroscopic features in other regions.

An interpretation more consistent with measured impurity levels, as well as crystallographic, spin-resonance, and annealing data is to attribute the broad IR absorption in $\text{Ti:Al}_2\text{O}_3$ to Ti^{3+} in low symmetry sites, most likely caused by adjacent point defects. In examining this interpretation, we must consider the formation and maintenance of point defects in Al_2O_3 .

The ubiquity of point defects in pure sapphire has long been established. Dils²⁴ has estimated the cationic defect concentration in pure (undoped) Al_2O_3 to be 10^{-4} and 10^{-7} of available lattice sites, for Frenkel and Schottky defects, respectively. Overall charge neutrality suggests a concentration of anionic Schottky defects (oxygen vacancies) of the same order. The number of oxygen interstitials is expected to be relatively small²⁵. When sapphire is doped with titanium, the defect situation is complicated considerably²⁶. Incorporation of TiO_2 into the melt has the double effect of increasing the anion to cation ratio in the melt, while fostering the formation of oxygen vacancies to charge compensate the tetravalent cation²⁷. Once titanium is reduced to the trivalent state, a whole new set of factors arise which will tend to increase the number of defects. The Ti^{3+} ions can, for example, occupy aluminum sites vacated by interstitial Al^{3+} ions, promoting charge compensation by anion vacancies. By comparing the strain energy due to the incorporation of Ti^{3+} into an Al^{3+} site⁶, with the energies required to form anion or cation

vacancies, we expect a vacancy concentration a few percent times the Ti^{3+} concentration due just to this factor.

Electron paramagnetic resonance (EPR) measurements confirm the presence of plentiful defects near Ti^{3+} ions in $Ti:Al_2O_3$. Early EPR studies^{28,29} indicated that in $Ti:Al_2O_3$ the g-factor perpendicular to the c-axis is non-zero, indicating that Ti^{3+} does not enter the lattice exactly substitutionally for Al^{3+} . The EPR lineshape of $Ti:Al_2O_3$ is broad, asymmetric, and weakly varying with angle, suggesting a random (both in direction and strength) inhomogeneous broadening. Bates, et.al.^{30,31}, accounted for this lineshape by estimating a concentration of singly charged point defects of 20 ppm, or a smaller number of multiply charged defects, in a crystal of Ti concentration 80 ppm. Random imperfections of the lattice, (such as stacking faults, and dislocations) and strain also contribute to the linewidth.

To test the effect of annealing on IR absorption, a comparison was made between two pieces of $Ti:Al_2O_3$, obtained by halving a slice taken across the boule. Both pieces initially have identical concentrations of dopant, scattering centers, impurities, defects, etc. The difference between the "as grown" sample, and the sample annealed at high temperature in an atmosphere which provides proper oxygen stoichiometry³² is visible even to the naked eye. The "as grown" sample is dulled by scattering centers (apparently small bubbles), and it has a slight bluish cast from the red end of the IR absorption of the IR absorption. The annealed sample is clearer, and pinker, with no visible blue tint. Accordingly, the absorption spectra show a decrease in background absorption and in the IR band, and an increase in blue-green

absorption (Fig. 2). In addition, on annealing, the edge of the UV absorption shifts by few nanometers to shorter wavelength. The annealed sample shows an increase in the deep red fluorescence, a decrease in yellow color center fluorescence, but an increase in violet fluorescence. Overall, color center emission drops substantially.

Relating specific changes in the spectra to specific types of defects is difficult with the available data. The reduction in IR absorption is probably a combination of reduction in adjacent point defects (O^{2-} vacancies, color centers, aluminum interstitials or vacancies, etc.) and the relaxation of Ti^{3+} from interstitial or defect sites into the desired Al^{3+} sites. The increase in blue-green absorption may be due to an increase of Ti^{3+} in high symmetry sites from the above effects, and to the reduction of Ti^{4+} ("as grown" crystals probably contain some Ti^{4+}) to Ti^{3+} .

The sensitivity of the individual ion absorption cross-sections to their sites further complicates the interpretation of annealing data. Since the ${}^2T_2 \rightarrow {}^2E$ transition is electric dipole allowed by the odd parity crystal field components, ions in grossly distorted sites, where the odd parity components are a strong perturbation, are expected to have a larger cross-section (by perhaps an order of magnitude) than an ion in, for example, an aluminum site without nearby point defects.

The broad wavelength range of the IR absorption is likely due to the range of field strengths and symmetries. In normal Al^{3+} sites, the low symmetry perturbations due to the Jahn-Teller and trigonal distortions are about one tenth of the strength of the octahedral field¹³. In a site where

the trigonal field is a larger perturbation, the splitting of the 2T_2 into A_1+E would be much larger, giving a double absorption at longer and shorter wavelengths compared to the absorption by the ion in an octahedral-dominated site i.e., the normal Al^{3+} site. An ion in an interstitial site, where the dominant symmetry is likely to be tetrahedral³³, would be expected to absorb at energies around one half that of the octahedrally coordinated Ti^{3+} . A three-fold axis is present in both of these cases, so the Jahn-Teller splitting would still be present. The shorter wavelength component of the trigonal field doublet may be part of the pronounced violet tail of the blue-green absorption.

III. Lasing

The preceding discussion of $Ti:Al_2O_3$ has suggested some of the material's strengths and weaknesses as a laser. The broad tuning range, the 4-level nature of the vibronic transition, the high gain, and the rugged host contrast with the short spontaneous emission lifetime, and the difficulty of obtaining high concentration, high quality crystals. Recent experiments have illustrated some of these aspects of $Ti:Al_2O_3$, and their effect on its usefulness as a laser.

The most unusual feature of $Ti:Al_2O_3$ is its very broad tuning range. The large overlap between the titanium and ligand orbitals strongly couples the Ti^{3+} ion to lattice vibrations. The material has lased from about 660 nm to 990 nm, with lasing beyond 1 μm expected in lower loss material. The high gain of $Ti:Al_2O_3$ allows a choice of tuning elements; we have used gratings, filters, prisms, and birefringent filters, with best results obtained using the latter because of its low insertion loss. Because the predominant broadening for lasing Ti^{3+} ions is homogeneous, the laser line can be narrowed to moderate linewidths with minimal loss in energy.

Efficient 4-level laser operation in $\text{Ti:Al}_2\text{O}_3$ occurs because the pump and lasing transitions mostly take place to high lying vibrational levels in the excited and ground manifolds, respectively, which relax to lower vibrational states approximately 10^6 times faster than the radiative decay rate. Thus, lasing takes place primarily due to transitions from the lowest vibrational states of the ^2E manifold, to excited vibrational states of the $^2\text{T}_2$ manifold. The threshold is therefore relatively low, and in part because the quantum efficiency is approximately unity up to about 400°K ,³⁴ no cryogenic cooling is required for efficient operation.

The high gain of $\text{Ti:Al}_2\text{O}_3$ (high for a vibronic laser in this wavelength range) is directly related to short fluorescent lifetime, so that it is both a positive feature and a negative feature. The high gain allows the use of high transmission output couplers at reasonable thresholds, resulting in high slope efficiency. The short lifetime makes flashlamp pumping substantially more difficult than with other transition metal lasers, like ruby and alexandrite.

The UV and IR absorptions in $\text{Ti:Al}_2\text{O}_3$ greatly limit laser performance. The UV absorption prevents the co-doping of laser rods to convert UV into blue-green, in order to increase flashlamp-pumped efficiency. The IR absorption keeps the threshold in $\text{Ti:Al}_2\text{O}_3$ at least an order of magnitude higher than it would otherwise be. With a loss at laser wavelengths of greater than $1\%/cm$ in our best $\text{Ti:Al}_2\text{O}_3$ rod, we measure a flashlamp-pumped laser threshold for a $10\text{ cm} \times 0.63\text{ cm}$ rod (with fluorescent converter)³⁵ of about 20 joules into the flashlamp. Simple scaling suggests a threshold of about 2 joules for a rod with a loss of $0.1\%/cm$ (comparable to that obtained in good quality

laser crystals). Improvements in flashtubes, drivers, and fluorescent converters could reduce the threshold for a flashlamp-pumped $\text{Ti:Al}_2\text{O}_3$ to below a joule, and increase slope efficiency from our present value of about 0.5%, to a few percent.

IV. Conclusion

We have outlined some of the problems in growing high quality, heavily doped $\text{Ti:Al}_2\text{O}_3$. While some of these problems will remain intrinsic to the medium, others can be eased through research into the growth of $\text{Ti:Al}_2\text{O}_3$ with better stoichiometry and fewer defects. The spectroscopy of $\text{Ti:Al}_2\text{O}_3$ will be better understood through more detailed optical and EPR studies of samples, as a function of growth conditions and annealing, paying particular attention to the incorporation of impurities. We expect these refinements to increase the already respectable performance of the $\text{Ti:Al}_2\text{O}_3$ laser.

References

1. P. Moulton, "Ti:Al₂O₃ - A New Solid State Laser", Solid State Research Report, Lincoln Laboratory, MIT (1982:3), pp. 15-21.
2. L. Esterowitz, R. Allen, and C. P. Khattak, "Stimulated Emission from Flashpumped Ti:Al₂O₃" in Tunable Solid State Lasers, Springer Series in Optical Sciences, 47, ed. by P. Hammerling, A. Budgor, and A. Pinto, Springer Verlag, Berlin 1985, pp. 73-75
3. G. F. Albrecht, J. M. Eggleston, and J. J. Ewing, "Measurements of Ti³⁺:Al₂O₃ as a Lasing Material", Optica Comm. 52, n6, Jan. 15, 1985, pp. 401-404.
4. R. D. Shannon and C. T. Prewitt, "Effective Ionic Radii in Oxides and Fluorides", Acta. Cryst. B25 (1969), pp. 925-946.
5. S. C. Abrahams, "Magnetic and Crystal Structure of Titanium Sesquioxide", Phys. Rev. 130, n6, 15 June 1963, pp. 2230-2237.
6. S. K. Roy and R. L. Coble, "Solubilities of Magnesia, Titania and Magnesium Titanate in Aluminum Oxide", J. Amer. Ceram. Soc., 51, n1, Jan 21, 1968, pp. 1-6.
7. Philipp H. Klein, private communication.
8. P. George and D. S. McClure, "The Effect of Inner Orbital Splittings on the Thermodynamic Properties of Transition Metal Compounds and Coordination Complexes," in F. A. Cotton (ed) Progress in Inorganic Chemistry, 1, Interscience, New York, 1959, pp. 381-464.
9. D. S. McClure, "The Effects of Inner Orbitals on Thermodynamic Properties", in Some Aspects of Crystal Field Theory, by T. S. Dunn, D. S. McClure, and R. G. Pearson, Harper and Row, New York, 1965, pp. 77-95.
10. A. Miller, "Distribution of Cations in Spinel", J. Appl. Phys. 30, n4, April 1959, pp. 24S-25S
11. D. S. McClure, "The Distribution of Transition Metal Cations in Spinel", J. Phys. Chem. Solids, 3, pp. 311-317.
12. J. S. Griffith, The Theory of Transition Metal Ions, Cambridge Univ. Press, Cambridge, 1961.
13. D. S. McClure, "Optical Spectra of Transition-Metal Ions in Corundum", J. Chem. Phys. 36, n10, May 15, 1962, pp. 2757-2779.

14. B. P. Gatcher and J. A. Koningstein, "Zero Phonon Transitions and Interacting Jahn-Teller Phonon Energies from the Fluorescence Spectrum of $\alpha\text{-Al}_2\text{O}_3\text{:Ti}^{3+}$ ", J. Chem. Phys. 60, n5, March 1, 1974, pp. 2003-2006.
15. N. F. Mott and R. W. Gurney, Electronic Processes in Ionic Crystals, Oxford University Press, London, 1948, pp. 95-99.
16. C. K. Jorgensen, "Some Problems of Intensity of Absorption Bands and Chemical Bonding," Acta. Chem. Scand. 9, n3, 1955, pp. 405-411.
17. H. H. Tippins, "Charge-Transfer Spectra of Transition-Metal Ions in Corundum" Phys. Rev. B, 1, n1, Jan 1, 1970, pp. 126-135.
18. J. Ferguson and P. E. Fielding, "The Origins of the Colours of Yellow, Green, and Blue Sapphires," Chem. Phys. Lett. 109, n3, August 1, 1971, pp. 262-265.
19. Gerhard Lehmann and Hermann Harder, "Optical Spectra of Di- and Tri-valent Iron in Corundum", Amer. Min. 55, Jan-Feb 1970, pp. 98-105.
20. T. S. Bessonova, M. P. Stanislavskii, and V. Ya. Khaimov-Malhov", "Effect of Heat Treatment and Irradiation on Absorption Spectra of Ti and Si Corundum", Opt. Spektrosk. 41, July 1976, pp. 152-154.
21. P. Moulton, private communication.
22. B. G. Draeger and G. P. Summers, "Defects in Unirradiated $\alpha\text{-Al}_2\text{O}_3$ ", Phys. Rev. B, 19, n2, Jan 15, 1979, pp. 1172-1177.
23. K. H. Lee and J. H. Crawford, Jr., "Electron Centers in Single-Crystal Al_2O_3 ", Phys. Rev. B, 15, n6, April 15, 1977, pp. 4065-4070.
24. R. R. Dils, "Cation Interdiffusion in the Chrome-Alumina System", Ph.D. Thesis, Stanford University, June 1965, 188 pp.
25. C. J. Dienes, D. O. Welch, C. R. Fischer, R. D. Hatcher, O. Lazareth;, and M. Samberg, "Shell Model Calculations of Some Point-Defect Properties in $\alpha\text{-Al}_2\text{O}_3$ ", Phys. Rev. B, 11, n8, April 15, 1975, pp. 3360-3370.
26. J. J. Rasmussen and W. D. Kingery, "Effect of Dopants on the Defect Structure of Single-Crystal Aluminum Oxide", J. Amer. Ceram. Soc. 53, n8, August 1970, pp. 436-440.
27. S. K. Mohapatra and F. A. Kroger, "Defect Structure of $\alpha\text{-Al}_2\text{O}_3$ Doped with Titanium", J. Amer. Ceram. Soc. 60, n9-10, Sept-Oct 1977;, pp. 381-387.

28. L. S. Kornienko and A. M. Prokhorov, "Electronic Paramagnetic Resonance of the Ti^{3+} Ion in Corundum", J. Exptl. Theoret. Phys. (USSR) 38, May 1960, pp. 1651-1652.
29. L. S. Kornienko, P. P. Pashinin, and A. M. Prokhorov, "The Spin-Lattice Relaxation Time of the Ti^{3+} Ion in Corundum", J. Exptl. Theoret. Phys. (USSR) 42, Jan 1962, pp. 65-66.
30. C. A. Bates and J. P. Bentley, "Lattice-Ion Interactions of Ti^{3+} in Corundum; I. The Jahn-Teller Effect and the Theory of the Effects of Electric Field and Strain", J. Phys. C (Solid State Physics), Ser. 2, 2, 1969, pp. 1947-1963.
31. C. A. Bates, J. P. Bentley, B. F. Jones, and W. S. Moore, "Lattice-Ion Interactions of Ti^{3+} in Corundum; III Analysis of the Electron Paramagnetic Resonance Lineshape", J. Phys. C. 3, 1970, pp. 570-578.
32. Union Carbide proprietary process.
33. R.W.G. Wyckoff, Crystal Structures, John Wiley and Sons, 1964, Chapter V, "Structures of Complex Binary Compounds R_nX_n ", pp. 6-8.
34. J. K. Tyminski, private communication.
35. P. Lacovara, L. Esterowitz and R. Allen, "Flashpumped $Ti:Al_2O_3$ Laser Using Fluorescent Conversion", Optics Letters, June, 1985 (to be published).

Figure Captions

- Fig. 1. Fluorescence of $\text{Ti:Al}_2\text{O}_3$ with excitation at different wavelengths: curve "a" from excitation at 253.7 nm, curve "b" from excitation at 313 nm; curve "c" from excitation at 454 nm. The curves are on different intensity scales for ease of presentation.
- Fig. 2. Absorption spectra of $\text{Ti:Al}_2\text{O}_3$ before and after annealing in controlled atmosphere.

